Neuron
Report

Hippocampal CA3 Output Is Crucial for Ripple-Associated Reactivation and Consolidation of Memory

Toshiaki Nakashiba,[1,2] Derek L. Buhl,[1,2] Thomas J. McHugh,[1,2,3] and Susumu Tonegawa[1,*]
[1]The Picower Institute for Learning and Memory, The RIKEN-MIT Center for Neural Circuit Genetics, Howard Hughes Medical Institute, Department of Biology and Department of Brain and Cognitive Sciences, Massachusetts Institute of Technology, Cambridge, MA 02139, USA
[2]These authors contributed equally to this work
[3]Present address: Laboratory for Circuit and Behavioral Physiology, RIKEN Brain Science Institute, 2-1 Hirosawa, Wako-shi, Saitama 351-0198, Japan
*Correspondence: tonegawa@mit.edu
DOI 10.1016/j.neuron.2009.05.013

SUMMARY

A widely held memory consolidation theory posits that memory of events and space is initially stored in the hippocampus (HPC) in a time-limited manner and is consolidated in the neocortex for permanent storage. Although posttraining HPC lesions result in temporally graded amnesia, the precise HPC circuits and mechanisms involved in remote memory storage remain poorly understood. To investigate the role of the trisynaptic pathway in the consolidation process we employed the CA3-TeTX transgenic mouse, in which CA3 output can be specifically and inducibly controlled. We found that posttraining blockade of CA3 output for up to 4 weeks impairs the consolidation of contextual fear memory. Moreover, in vivo hippocampal recordings revealed a reduced intrinsic frequency of CA1 ripples and a significant decrease in the experience-dependent, ripple-associated coordinated reactivation of CA1 cell pairs. Collectively, these results suggest that the posttraining integrity of the trisynaptic pathway and the ripple-associated reactivation of hippocampal memory engram are crucial for memory consolidation.

INTRODUCTION

In both human and animals damage to the hippocampus following learning results in temporally graded impairment of long-term memory (Anagnostaras et al., 1999; Kim and Fanselow, 1992; Squire, 1992). A widely held explanation for these behavioral and clinical data is that over time the episodic, contextual, or spatial memory initially stored in the HPC (recent memory) is consolidated to the neocortex for permanent storage (remote memory), thus making the HPC dispensable for its recall and expression (Frankland and Bontempi, 2005; McClelland et al., 1995; Squire and Alvarez, 1995; Teyler and Rudy, 2007). Although there remain uncertainties regarding the relative contributions of the HPC and neocortex as the storage sites of recent and remote memories (Buzsaki, 1996; Clark et al., 2007; Lehmann et al., 2007; Martin et al., 2005; Nadel and Moscovitch, 1997), there is agreement among various consolidation models that interaction between the HPC and neocortex after the experience and formation of recent memory is crucial for the consolidation process. However, little is known as to which HPC circuit is important for this interaction.

The neuronal network of HPC and its adjacent cortex, entorhinal cortex (EC), contains two major excitatory circuits, the trisynaptic pathway (EC layer II → dentate gyrus → CA3 → CA1 → EC layer V) and the direct pathway (EC layer III → CA1 → ECV), that converge onto a common HPC output structure, the CA1 region (Amaral and Witter, 1989). Here, we investigate whether, after the encoding of a memory in the HPC, continued output from CA3 via the trisynaptic pathway is necessary for systems consolidation of this memory. This issue is particularly important because, despite the fact that the CA3 recurrent network is thought to be a major storage site for recent HPC memory (Marr, 1971; Rolls and Kesner, 2006), recent work has shown that the alternative direct pathway that bypasses CA3 is necessary for the consolidation process (Remondes and Schuman, 2004). We addressed this issue by taking advantage of the CA3-TeTX inducible transgenic mouse in which blockade of CA3 output could be targeted only to the posttraining period following contextual fear conditioning (Nakashiba et al., 2008). We found that the posttraining blockade of CA3 output via the trisynaptic pathway impairs consolidation of contextual fear memory.

Further, we employed in vivo multiple tetrode recordings to the CA3-TeTX mice to obtain physiological correlates of the behavioral deficits. Specifically, we investigated whether high frequency field oscillations ("ripples") in CA1 as well as the ripple-associated reactivation of experience-related firing patterns of CA1 pyramidal cells were impaired in the mutants. Previous studies hypothesized that these physiological processes may be involved in the consolidation process, but evidence has been lacking (Buzsaki, 1989, 1996; Ji and Wilson, 2007; Lee and Wilson, 2002; Siapas and Wilson, 1998; Skaggs and McNaughton, 1996; Wilson and McNaughton, 1994). Our data showed that in the CA3-TeTX mice the intrinsic frequency of ripples and the reactivation were both reduced significantly, supporting the hypothesis that these physiological processes are crucial for memory consolidation.

RESULTS AND DISCUSSION

We previously established that in the CA3-TeTX transgenic mice CA3 output is normal while the animals are raised on a diet containing doxycycline (Dox) but becomes blocked following Dox

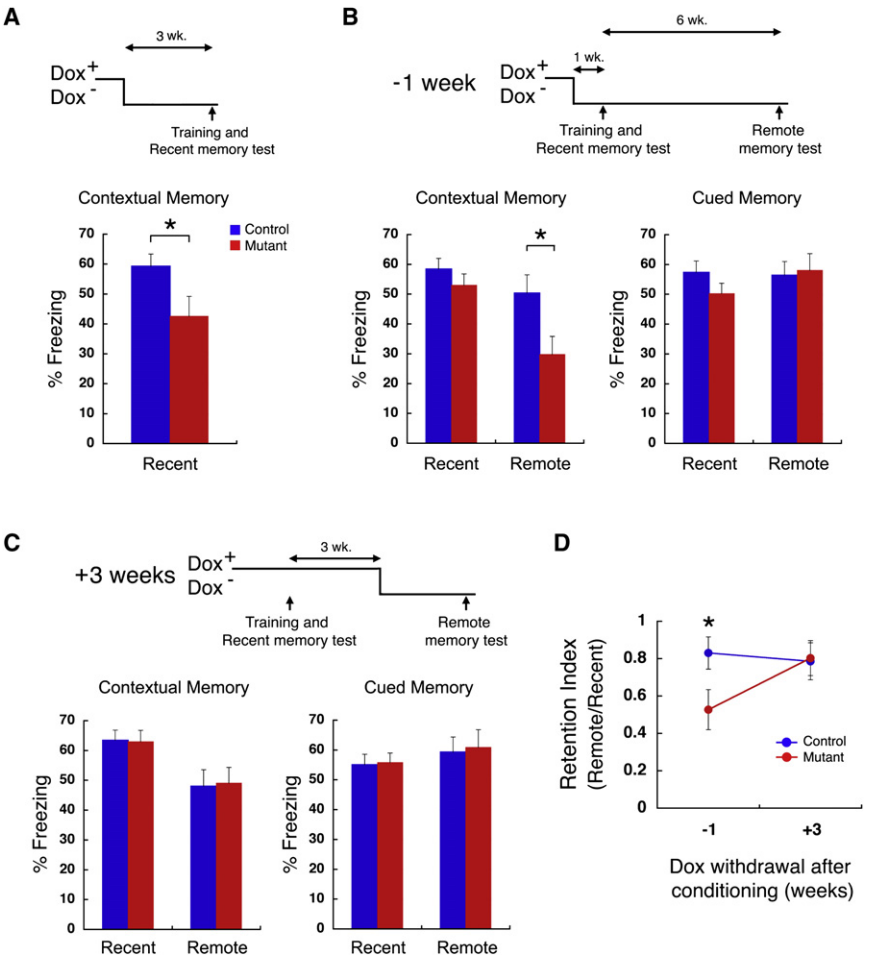

Figure 1. Consolidation of Contextual, but Not Cued Fear Memory, Is Impaired in CA3-TeTX Mice

(A) Averaged freezing levels during the recent contextual memory test following 3 weeks Dox withdrawal (control, blue bar; mutant, red bar; n = 12 per genotype). Mutants exhibited significantly less freezing ($p < 0.05$).

(B) Averaged freezing levels during the contextual and cued memory tests. Dox was withdrawn 1 week before training (−1 week), and recent and remote memories were tested (n = 24 per genotype). Mutant mice displayed significantly less freezing in the remote contextual memory test compared to the control littermates ($p < 0.05$), but not in the recent contextual memory test. In cued memory tests, mutants and controls showed similar freezing levels in both recent and remote memory tests.

(C) Averaged freezing levels during the contextual and cued memory tests. Dox was withdrawn three weeks after training (+3 weeks). Mutants exhibited no deficit in either recent or remote contextual or cued memory. Protocols for Dox^+ to Dox^- diet switches relative to the timing of training and memory tests are indicated at the top of (A)–(C).

(D) Freezing levels of individual mice during remote memory tests were divided by those during the remote memory tests (retention index) for contextual fear conditioning (control, blue circle; mutant, red circle; $p < 0.05$ for the −1 week protocol). Data shown as mean ± SEM.

withdrawal without the converging output to CA1 from the temporoammonic (TA) axons being affected (Nakashiba et al., 2008). More specifically, it requires 2 weeks of Dox withdrawal from the diet before any significant blockade of transmission occurs at the Schaffer collateral (SC)-CA1 synapses, while by the end of the third week of Dox withdrawal the field excitatory postsynaptic potential (fEPSP) at the SC-CA1 synapses is reduced by over 90% (Nakashiba et al., 2008). Under the latter conditions, no population spikes were induced, even after applying high-frequency stimulation to the SCs, suggesting that the residual transmission at the mutants' SC-CA1 synapses would not be able to induce action potentials in vivo in CA1 pyramidal cells (Nakashiba et al., 2008). Further, under these conditions, the CA3-TeTX mice were impaired in the acquisition of contextual fear memory (recent memory) when a 3 min exposure to a novel context was paired with a mild foot shock (one CS-US pair protocol; Nakashiba et al., 2008). For the present study, a stronger conditioning protocol composed of three CS-US pairs (see Experimental Procedures) was employed in order to study long-lasting memory (remote memory). We confirmed that normal SC input to CA1 is necessary for the acquisition of the full level of contextual fear memory in the 3 CS-US pair version of the task (Figure 1A).

We then targeted the blockade of the SC-CA1 transmission to the period following the training session in order to investigate its role in systems consolidation. For this purpose, we raised the CA3-TeTX mice on Dox diet and switched to a Dox-free diet 1 week prior to the fear conditioning training session, ensuring the SC input would be intact during memory acquisition but would cease about 1 week after training (Figure 1B). Recent and remote contextual memories were tested one day and six weeks after training in the same context, respectively, while recent and remote cued memories were tested in a distinct context 1 day after the corresponding contextual fear memory test. As expected, mutants did not exhibit a recent memory deficit in either contextual or cued conditioning (Figure 1B). In contrast, the mutants' remote fear memory was significantly reduced in the contextual (Figures 1B and 1D; $p < 0.05$ for both) but not in the cued conditioning task (Figure 1B). The remaining remote memory may be due to a delay in the completion of the posttraining blockade of the SC input and/or the residual, off-line reactivation of CA1 memory traces even under the complete blockade of CA3 output (see below).

The above experimental protocol did not allow us to determine if the observed deficit in remote contextual memory was due to a deficit in either or both the consolidation and/or recall process. To distinguish these possibilities, we subjected a second set of mice to fear conditioning; however, in this case withdrawing Dox 3 weeks after training (Figure 1C). Because there is no

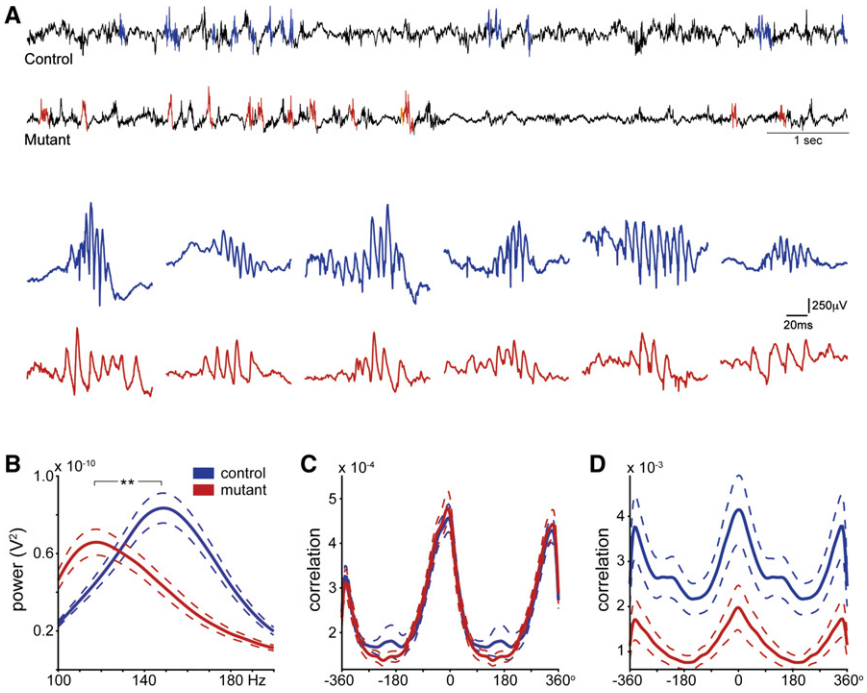

Figure 2. Loss of CA3 Output to CA1 Results in a Decrease in the Intrinsic Frequency of Ripple Oscillations

(A) LFP samples from control (top) and mutant (bottom) mice during SQ periods. Detected ripples are highlighted in either blue (control) or red (mutant). Below the LFP traces are individual ripple examples from six randomly selected controls (blue) and mutants (red). Note the clear decrease in the mutant ripple intrinsic frequency.

(B) The amplitude of ripples is not altered in mutants; however, there was a significant decrease in the intrinsic frequency of mutant (n = 12) ripples compared to controls (n = 14; p = 4.31e-19).

(C and D) Both phase preference and probability of firing of pyramidal cells (C) were consistent between mutants and controls. Although the phase preference of interneurons did not change in the mutants, the probability of firing was significantly lower in the mutants (D; p = 0.006). Data shown as mean ± SEM.

significant reduction of the SC input up to 2 weeks after Dox withdrawal (Nakashiba et al., 2008), the mutant mice treated this way have had a total of 5 weeks with an intact SC input following the training, a period sufficient for a full consolidation of recent memory (Kim and Fanselow, 1992). On the other hand, the SC input is blocked over 90% at 3 weeks after Dox withdrawal (Nakashiba et al., 2008), which corresponds to 6 weeks after the training, the time point of the remote memory test. Under this protocol, we did not observe a deficit in either contextual or cued remote memories (Figures 1C and 1D) in the mutants. Together, these experiments suggest that while CA3 output is not required for recall of a remote contextual fear memory, it plays a crucial role in the consolidation of the memory for a period of several weeks following training, but not beyond.

It has been hypothesized that high frequency synchronized field oscillations (“ripples”) observed in CA1 during slow wave sleep or awake quiescent periods (hereafter referred to as SQ periods) and the ripple-associated, off-line “reactivation” of experience-dependent coordinated activity patterns of CA1 cells are crucial for memory consolidation (Buzsaki, 1996; Ji and Wilson, 2007; Lee and Wilson, 2002; Siapas and Wilson, 1998; Skaggs and McNaughton, 1996; Wilson and McNaughton, 1994). As possible neurophysiological correlates of the observed behavioral consolidation deficit, we examined ripples and ripple-associated reactivation in the CA3-TeTX mice. For this purpose we used multiple-tetrode drives to record both the local field potential (LFP) and single unit activity from mice as they explored a novel linear track (RUN), as well as during SQ periods that bracketed the RUN session (PRE and POST, respectively). In control mice, the dominant high-frequency oscillations during SQ periods had an average intrinsic frequency of 148.84 ± 1.57 Hz, resembling classically defined ripples (Buzsaki et al., 1992; O’Keefe and Nadel, 1978; Figures 2A and 2B). In the mutant mice, the lack of CA3 output did not alter the number of high-frequency oscillations meeting ripple criteria (control 0.65 ± 0.07 ripples/s; mutant 0.48 ± 0.05 ripples/s; see SOM) but did result in a significant reduction of the average intrinsic frequency (119.50 Hz ± 1.77 Hz; $p < 0.001$) of the oscillations, with the majority (~80%) of events ranging between 110–125 Hz (Figures 2A and 2B). We did not see a reduction in the length of ripple oscillations in mutant animals compared to controls (42.30 ± 5.38 ms versus 48.62 ± 5.56 ms, respectively); however, there was a significant reduction in the number of wavelets per ripple epoch in the mutants (4.04 ± 0.49 versus 2.32 ± 0.41, $p < 0.01$). Hereafter, for brevity we refer to the control and mutant oscillations as fast and slow ripples, respectively, or sometimes both simply as ripples.

We next examined the spiking properties of individual pyramidal cells and interneurons during SQ periods to assess the cell types participating in the generation of ripples. There was no difference between genotypes in the mean firing rate of pyramidal cells, in the complex spike index (CSI; a measure of bursting [Nakazawa et al., 2002]) or in the mean burst length, although there was a small decrease in the fraction of spikes participating in bursts in the mutant (Table 1). Interneurons in the mutants, however, fired significantly less during SQ periods (Table 1), including during ripple episodes (Figure 2D). Similar to past reports (Csicsvari et al., 1999), in both genotypes, pyramidal cells tended to fire on the trough of ripple wavelets while interneurons fired slightly before or after (Figures 2C and 2D). This suggests that although ripples in the mutants are significantly slower than those in controls on average, the field oscillations observed in CA1 are likely generated via similar mechanisms; namely a strong synchronous depolarization that is coupled with rapid perisomatic inhibition mediated through the local interneuron network (Ylinen et al., 1995). The source of these excitatory inputs in the mutants may be the TA input from the EC layer III and/or the input from the nucleus reuniens of the thalamus (TR input; Wouterlood

Table 1. Firing Properties of CA1 Pyramidal Cells and Interneurons during SQ Periods

	Control (N = 14, n = 94)	Mutant (N = 12, n = 91)
Pyramidal Cells		
Mean firing rate (Hz)	0.789 ± 0.08	0.90 ± 0.09
Complex spike index (bursting)	29.20 ± 1.62	28.93 ± 1.47
Fraction of spike in bursts (% total)	37.9 ± 1.23	34.5 ± 1.06*
Mean burst length (# of spikes)	2.16 ± 0.06	2.14 ± 0.07
	Control (N = 15, n = 56)	Mutant (N = 13, n = 75)
Interneurons		
Mean firing rate (Hz)	9.34 ± 1.00	4.61 ± 0.68**
Complex spike index (bursting)	1.51 ± 0.43	1.94 ± 0.50

We examined the spiking activity during SQ periods of high spatial information pyramidal cells and interneurons recorded in area CA1. We found a small, yet significant decrease in the fraction of spikes that participated in bursts in mutant mice; however, no differences were observed in CSI, mean rate or mean burst length. Interestingly, interneurons in mutants showed a significant decrease in mean firing rate during SQ periods. N, number of mice; n, number of cells. *p = 0.042; **p < 0.001.

et al., 1990). The appearance of slow ripples, coupled with reduced inhibition in the mutants may reflect a change in the numbers or types of interneurons recruited in the absence of SC input. Alternatively, the decrease in inhibitory tone resulting from SC blockade may have revealed the previously hypothesized ability of the CA1 network to generate intrinsic oscillations in the slow ripple frequency range (Buzsaki et al., 1992) alone or in conjunction with TA/TR input.

While ripples reflect the synchronous discharge of CA1 pyramidal cells and interneurons, it is hypothesized that the key to synaptic plasticity and memory consolidation is the specific coactivation of subsets of cells that reflect the neuronal activity present during learning (Foster and Wilson, 2006; Kali and Dayan, 2004). Previous work has demonstrated that pairs of neurons that are spatially correlated in firing during behavior (RUN) exhibited higher temporal correlations following the experience (POST) compared to the SQ periods preceding it (PRE) (reactivation). We have previously shown that CA1 neurons in CA3-TeTX mice have, on average, poorer spatial specificity than control neurons, particularly in a novel space (Nakashiba et al., 2008). To focus our experiment on the memory consolidation phase, we limited our reactivation analysis to pyramidal cells with robust place fields in both genotypes based on their spatial information value and average firing rate (see Table S1 available online; see Experimental Procedures). We classified pairs of simultaneously recorded cells by the degree of spatial overlap of their fields as overlapping (50% or greater spatial overlap; representative examples shown in Figures 3A and 3B) or nonoverlapping (no spatial overlap; representative examples shown in Figures 3C and 3D). There were no significant differences between genotypes in the average amount of overlap or in the temporal correlations during run of the overlapping pairs. Further, we observed a significant correlation between the spatial overlap measure and the temporal correlation of the cell's firings during behavior in both genotypes (Table S2). When looking for increased correlations of overlapping cell pairs during POST relative to PRE (Δ correlation) outside of ripples, no increase was observed in either control or mutant mice (data not shown). We then calculated the degree of correlation in the firing of cell pairs during all ripple epochs that occurred before (PRE) and after (POST) spatial exploration and determined the difference between them (Δ correlation). Consistent with earlier work (Wilson and McNaughton, 1994), overlapping pairs in control mice showed an increased correlation of firing during POST-run ripples compared to PRE-run ripples (Figures 3A and 3E), while nonoverlapping pairs showed no change (Figures 3C and 3E). This increase of coordinated firing between overlapping cell pairs was significantly reduced in the mutants, suggesting impairment in the off-line reactivation of neuronal ensembles in a manner reflecting the animals' experience (Figures 3B and 3E). Thus, while the firing of CA1 pyramidal cells remain phase locked during ripples (Figure 2C) in the absence of the SC input, this activity does not reflect previous experience as well as it does in the presence of SC input.

While experience-dependent coactivation of overlapping pairs was clearly reduced in mutants, it was still higher than that of nonoverlapping pairs (Figure 3E). This may in part be due to the remaining ripple events still present in mutants in which the intrinsic oscillation frequency was within the range of control ripples. To test this hypothesis, we calculated the Δ correlation values only for spikes occurring during ripples whose dominant intrinsic frequency was in the top 15% (i.e., those that fell within the control ripple frequency band; see Experimental Procedures) and found no significant genotype-specific differences (Figure 3F). This indicates that the minority of ripple events with high intrinsic frequency present in mutants are capable of supporting off-line reactivation of experience-related neuronal ensembles, which may have contributed to the remaining remote memory (Figures 1B and 1D). Further, we observed a significant decrease in spatial information (bits/spike) in the selected mutant cells (Table S1). To ensure this decrease did not bias the deficit in off-line reactivation, we removed cell pairs from either the highest quality control pairs, the lowest quality mutant pairs or both to the point in which the significant decrease was no longer observed (i.e., $p > 0.1$). With these limitations, we did not find a relationship between the degree of ripple related reactivation and spatial information in either genotype (Table S3).

Here, we demonstrated that blockade of CA3 output targeted to a posttraining period of about four weeks led to a specific deficit in the remote memory of contextual fear without affecting its recall or the remote memory of cued fear. These results suggest that the continued CA3 output and the integrity of the trisynaptic pathway after the formation of recent memory in the HPC is important for consolidation of contextual fear memory for a limited period of up to about 4 weeks, but not beyond. Our results do not exclude the possibility that other hippocampal pathways also contribute to consolidation of hippocampal dependent memory. For instance, the parallel direct pathway, which bypasses CA3, was shown to be crucial for the consolidation of a HPC-dependent spatial memory in a recent study carried out on rats with the electrolytic lesions of TA axons (Remondes and Schuman, 2004). In that study, however, the area affected

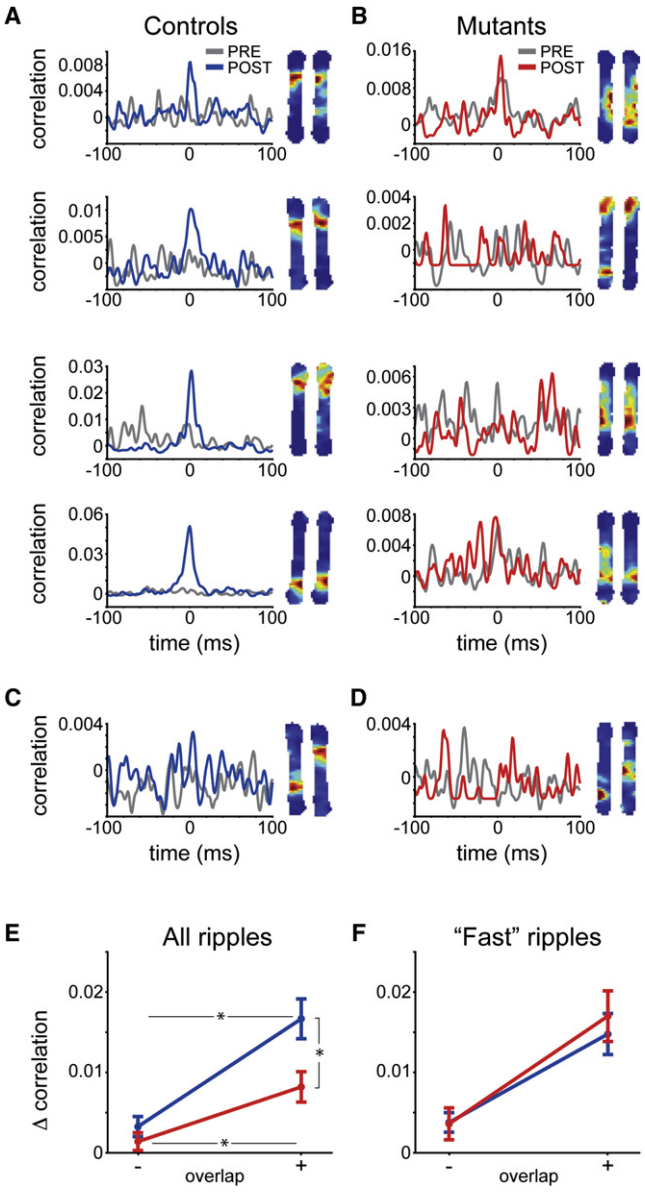

Figure 3. Blockade of CA3 to CA1 Transmission Results in a Loss of Reactivation during Postbehavior SQ Periods

(A and B) Representative examples of control (left) and mutant (right) cell pair correlations during prerun and postrun SQ periods. Heat maps (right of graphs) illustrate the spatial overlap between the two cells in the novel environment. Note that although the place fields of Mutant cells had significant overlap, little or no increase in their pairwise correlation was observed during post-SQ periods.

(C and D) Representative examples of cell pair correlations for cells with nonoverlapping place fields. Note the lack of pairwise correlation increase during post-SQ periods for both controls and mutants.

(E) Quantification of all pair-wise correlations during ripple epochs (control: 91 cells from 14 mice, overlapping pairs = 98, nonoverlapping pairs = 229; mutant: 94 cells from 12 mice, overlapping pairs = 132, nonoverlapping pairs = 215). Both genotypes show a significant increase in correlation when their place fields overlap and when taking all ripples into account. Note the significant reduction in Δ correlation (post-SQ periods correlation − pre-SQ periods correlation) in mutant (red line) animals compared to controls (blue line two-way analysis of variance, genotype × overlap $F(1670 = 3.96$, $p = 0.047$; Bonferroni posttests: control nonoverlapping × overlapping, $p < 0.001$; CA3-TeTX nonoverlapping × overlapping, $p < 0.01$; control overlapping × CA3-TeTX overlapping, $p < 0.01$).

(F) Evaluation of reactivation during ripples only falling into the average Control ripple frequency. When mutant ripples were in the average control ripple frequency range, the deficit in Δ correlation was not observed. Data shown as mean ± SEM.

by the lesion may have extended to the subiculum, impacting CA1 output and hence blocking, at least partially, the trisynaptic pathway. Nevertheless, it is possible that both trisynaptic and direct pathways contribute to the consolidation process.

Our present work also demonstrated that a highly specific blockade of CA3 output to CA1 resulted in reductions in the intrinsic oscillation frequency of ripples in CA1 as well as a significant decrease in the experience-dependent enhancement of the ripple-associated coordinated reactivation of CA1 cell pairs during postrun SQ periods. When combined with the behavioral deficit observed in the same mutant mice, these results suggest that ripples with high oscillation frequencies and ripple-associated reactivation of experience-related neuronal firing patterns during SQ periods play a crucial role in the consolidation of hippocampal-dependent recent memories into a remote memory that no longer requires CA3 drive. Although the physiological and behavioral deficits observed in mutant mice are correlatory, the association is strengthened by the exquisite specificity of the genetic intervention method employed (Nakashiba et al., 2008). In contrast, the possible role of ripples and ripple-associated reactivation or replay in memory consolidation was previously inferred only on the grounds that such physiological activities would strengthen synaptic plasticity at various sites downstream of CA1, including some cortical regions (Buzsaki, 1989; Foster and Wilson, 2006; Ji and Wilson, 2007).

The intrinsic oscillation frequency of a minor fraction of mutant ripples was in the normal range and a fraction of the experience-dependent increase in the co-activation of CA1 cell pairs remained in these mice. While it could be argued that these remaining activities reflect "leakiness" in the blockade of transmission at SC-CA1 synapses, we believe this is unlikely because our earlier studies showed that residual synaptic transmission at SC inputs in mutants failed to elicit population spikes in the fEPSP at stimulation intensities far greater than that expected in vivo (Nakashiba et al., 2008). We believe that a more likely interpretation of the remaining high frequency ripples in the mutants is that in the absence of SC input, TA and/or TR input can trigger these ripples, albeit less consistently than SC input. Likewise, the remaining experience-associated correlation of CA1 cell pair firings suggest that the TA and/or TR input can provide experience-related information to CA1, albeit less efficiently than SC input. For instance, the multisite recurrent network CA1 → ECV → ECIII → CA1 (Naber et al., 2001) could associate and store a diverse set of information.

In summary, using a mutant mouse in which the CA3 to CA1 synaptic transmission can be specifically inhibited in a temporally controllable manner, we demonstrated the importance of postrecent memory integrity of the HPC trisynaptic pathway for memory consolidation. We also demonstrated that in the mutant mice,

CA1 ripples and the ripple-associated reactivation of experience-dependent firing patterns of CA1 neurons are impaired, supporting the hypothesis that these physiological mechanisms underlie the consolidation of HPC-dependent memory.

EXPERIMENTAL PROCEDURES

Animals

All the experiments were carried out by operators blind to the animal's genotype using male CA3-TeTX mice (strain C57BL/6) between 14 and 24 weeks of age and their control male littermates. The specificity, completeness, and time course of blockade of synaptic transmission in CA3-TeTX mice were reported previously (Nakashiba et al., 2008). Two to four mice were housed per cage under the conditions of a 12 hr light/dark cycle and ad libitum access to food and water. All procedures relating to animal care and treatment conformed to the Institutional and NIH guidelines.

In Vivo Electrophysiology

All experiments were performed by operators who were blind to the genotypes. Animals were implanted with a microdrive array consisting of six independently adjustable tetrodes (targeted to CA1: stereotaxic coordinates from bregma: 1.6 mm lateral; 1.8 mm posterior) as previously described (McHugh et al., 1996; Nakashiba et al., 2008). In brief, electrodes were slowly advanced over 1 week to reach the CA1 pyramidal cell layer, and recordings commenced once stable cells were present. Putative hippocampal cells and local field potential (LFP) were recorded during a 20–30 min SQ session before and after (PRE and POST SQ periods, respectively) a 10 min exposure to a novel linear track (~81 cm, RUN). Position and directionality was tracked using a pair of infrared diodes placed 3 cm above the animals' head and 3 cm front to back. To eliminate periods of immobility, only periods when the animals were running above 2cm/s were used for the pairwise correlation analysis. For SQ, only periods in which the animals were completely still for greater than 30 s were used. SQ periods were further determined using the theta/delta ratio (Csicsvari et al., 1999). After recordings were completed, mice were given a lethal dose of anesthetic and an electrical current (50 μA) was run down each tetrode for 8 s to create a small lesion at the tip of the probe. Animals were then transcardially perfused with 4% PFA in PB and brains were removed, coronal slices (50 μM thick) were prepared using a Vibrotome, mounted and finally counterstained with Nuclear Fast Red to visualize electrode tracks and lesion sites. Recording positions were verified by examination of the lesion sites under standard light microscopy.

Individual neurons were classified offline based on each action potential's relative amplitude across the four recording wires of a tetrode (McHugh et al., 1996). Cells were further classified as pyramidal cells or interneurons based on the average width of their waveforms, bursting properties, and autocorrelation histograms (Csicsvari et al., 1998). Given the previously reported encoding deficits in the CA3-TeTX mice (Nakashiba et al., 2008), we limited the reactivation analysis to cells in both genotypes that best represented the spatial environment. For inclusion, cells were required to have a spatial information index (bits/spike) of >0.5 and an average firing rate of >0.2 Hz on the linear track. Place fields were calculated by counting the number of spikes falling into 2 cm bins along the linear track. Bins that had a firing rate below 1 Hz and bins containing less than 10% of the spikes contained in the maximum bin were excluded in the overlap analysis. We then classified all cell pairs as overlapping or nonoverlapping based on the average place field location. Overlapping place fields were defined as cells firing on the linearized track with >50% overlapping bins. Nonoverlapping place fields were defined as those with 0% overlap, and all other pairs were discarded. Pairwise correlations during run were calculated in 10 ms bins ± 1000 ms. Pairwise correlations during SQ periods were calculated in 10 ms bins ± 100 ms from the peak of the ripple or outside of the ripple. Correlation peaks were calculated if the value at time 0 was 3 SD above the mean.

To verify that the criterion of spatial information content did not influence the reactivation properties of the control or mutant cell pairs, the data was segregated in three ways: (1) We removed only good control cell pairs to the point in which the spatial information content between controls and mutants was no longer significant ($p > 0.1$); (2) we removed only poor mutant cell pairs to the same point; and (3) we removed both good control cell pairs and poor mutant cell pairs to the same point.

Ripples were detected using modifications to methods previously described (Csicsvari et al., 1999). The LFP was band-pass filtered between 90 and 250 Hz using a Hamming-window based FIR filter. To extract ripple events, the power (root mean square) of the filtered data was quantified and the beginning, middle, and ends of ripple periods were classified for all epochs >5 SD. The troughs of individual ripple wavelets were then detected by finding the minimum points during each episode that were greater than 20% of the maximum peak amplitude. For cleaner detection of the power and peak frequency for each ripple, the multitaper method (Buhl et al., 2003) was performed on the filtered ripple epochs. "Fast" (>140 Hz) ripples were then classified using a ratio of the power between the 110–125 Hz and 140–180 Hz frequency bands. Only ripples with significantly higher power in the upper band were classified as "fast."

Behavioral Experiments

All experiments were performed by operators who were blind to the genotypes and Dox treatments. For fear conditioning, room and chamber settings were the same as previously described (Nakashiba et al., 2008). Training consisted of a single exposure to the conditioning context for 6 min, during which three pairs of tone and electrical foot shock were given. Once placed in the chamber, mice were allowed to freely explore for 3 min. We then played a 30 s tone (2 kHz; 70 db) that coterminated with a 1.00 mA foot shock (1 s in duration). The mice received two additional tone and shock pairings at an intertrial interval of 1 min. Following the last shock delivery, mice remained in the chamber for 30 s. A recent contextual fear memory test was conducted 24 hr later, when the mice were placed in the conditioning chamber for 3 min without any tone presentation. A recent tone fear memory was measured in a second distinct chamber 48 hr after the training. The same tone (2 min in duration) as the one used in the training session was delivered after the mice were placed in the second chamber for 3 min. Six weeks after the training session, a remote contextual fear memory test was conducted followed by a remote tone fear memory test on the next day. Procedures for the remote memory tests were the same as the ones used in the recent memory tests.

SUPPLEMENTAL DATA

Supplemental Data include three tables and can be found with this article online at http://www.cell.com/neuron/supplemental/S0896-6273(09)00388-2.

ACKNOWLEDGMENTS

We thank Akiyo Ogawa, Frank Bushard, Michael Ragion, Carl Twiss, Jayson Derwin, and Dina Rooney for technical help. We thank Dr. Fabian Kloosterman and Dr. Jennie Z. Young for advice, the members of the Tonegawa lab for discussion, Dr. Matt Wilson for providing advice and the recording facility, and Nayiri Arzoumanian for help with manuscript preparation. This work was supported by NIH grants R01-MH078821 and P50-MH58880 to S.T. We thank Otsuka Pharmaceutical Development & Commercialization Inc. (OPDC) for their gift to support this research.

Accepted: May 14, 2009
Published: June 24, 2009

REFERENCES

Amaral, D.G., and Witter, M.P. (1989). The three-dimensional organization of the hippocampal formation: a review of anatomical data. Neuroscience *31*, 571–591.

Anagnostaras, S.G., Maren, S., and Fanselow, M.S. (1999). Temporally graded retrograde amnesia of contextual fear after hippocampal damage in rats: Within-subjects examination. J. Neurosci. *19*, 1106–1114.

Buhl, D.L., Harris, K.D., Hormuzdi, S.G., Monyer, H., and Buzsaki, G. (2003). Selective impairment of hippocampal gamma oscillations in connexin-36 knock-out mouse in vivo. J. Neurosci. *23*, 1013–1018.

Buzsaki, G. (1989). Two-stage model of memory trace formation: a role for "noisy" brain states. Neuroscience *31*, 551–570.

Buzsaki, G. (1996). The hippocampo-neocortical dialogue. Cereb. Cortex *6*, 81–92.

Buzsaki, G., Horvath, Z., Urioste, R., Hetke, J., and Wise, K. (1992). High-frequency network oscillation in the hippocampus. Science *256*, 1025–1027.

Clark, R.E., Broadbent, N.J., and Squire, L.R. (2007). The hippocampus and spatial memory: findings with a novel modification of the water maze. J. Neurosci. *27*, 6647–6654.

Csicsvari, J., Hirase, H., Czurko, A., and Buzsaki, G. (1998). Reliability and state dependence of pyramidal cell-interneuron synapses in the hippocampus: an ensemble approach in the behaving rat. Neuron *21*, 179–189.

Csicsvari, J., Hirase, H., Czurko, A., Mamiya, A., and Buzsaki, G. (1999). Fast network oscillations in the hippocampal CA1 region of the behaving rat. J. Neurosci. *19*, RC20.

Foster, D.J., and Wilson, M.A. (2006). Reverse replay of behavioural sequences in hippocampal place cells during the awake state. Nature *440*, 680–683.

Frankland, P.W., and Bontempi, B. (2005). The organization of recent and remote memories. Nat. Rev. Neurosci. *6*, 119–130.

Ji, D., and Wilson, M.A. (2007). Coordinated memory replay in the visual cortex and hippocampus during sleep. Nat. Neurosci. *10*, 100–107.

Kali, S., and Dayan, P. (2004). Off-line replay maintains declarative memories in a model of hippocampal-neocortical interactions. Nat. Neurosci. *7*, 286–294.

Kim, J.J., and Fanselow, M.S. (1992). Modality-specific retrograde amnesia of fear. Science *256*, 675–677.

Lee, A.K., and Wilson, M.A. (2002). Memory of sequential experience in the hippocampus during slow wave sleep. Neuron *36*, 1183–1194.

Lehmann, H., Lacanilao, S., and Sutherland, R.J. (2007). Complete or partial hippocampal damage produces equivalent retrograde amnesia for remote contextual fear memories. Eur. J. Neurosci. *25*, 1278–1286.

Marr, D. (1971). Simple memory: a theory for archicortex. Philos. Trans. R. Soc. Lond. B Biol. Sci. *262*, 23–81.

Martin, S.J., de Hoz, L., and Morris, R.G. (2005). Retrograde amnesia: neither partial nor complete hippocampal lesions in rats result in preferential sparing of remote spatial memory, even after reminding. Neuropsychologia *43*, 609–624.

McClelland, J.L., McNaughton, B.L., and O'Reilly, R.C. (1995). Why there are complementary learning systems in the hippocampus and neocortex: insights from the successes and failures of connectionist models of learning and memory. Psychol. Rev. *102*, 419–457.

McHugh, T.J., Blum, K.I., Tsien, J.Z., Tonegawa, S., and Wilson, M.A. (1996). Impaired hippocampal representation of space in CA1-specific NMDAR1 knockout mice. Cell *87*, 1339–1349.

Naber, P.A., Lopes da Silva, F.H., and Witter, M.P. (2001). Reciprocal connections between the entorhinal cortex and hippocampal fields CA1 and the subiculum are in register with the projections from CA1 to the subiculum. Hippocampus *11*, 99–104.

Nadel, L., and Moscovitch, M. (1997). Memory consolidation, retrograde amnesia and the hippocampal complex. Curr. Opin. Neurobiol. *7*, 217–227.

Nakashiba, T., Young, J.Z., McHugh, T.J., Buhl, D.L., and Tonegawa, S. (2008). Transgenic inhibition of synaptic transmission reveals role of CA3 output in hippocampal learning. Science *319*, 1260–1264.

Nakazawa, K., Quirk, M.C., Chitwood, R.A., Watanabe, M., Yeckel, M.F., Sun, L.D., Kato, A., Carr, C.A., Johnston, D., Wilson, M.A., and Tonegawa, S. (2002). Requirement for hippocampal CA3 NMDA receptors in associative memory recall. Science *297*, 211–218.

O'Keefe, J., and Nadel, L. (1978). The Hippocampus as a Cognitive Map (Oxford: Clarendon Press).

Remondes, M., and Schuman, E.M. (2004). Role for a cortical input to hippocampal area CA1 in the consolidation of a long-term memory. Nature *431*, 699–703.

Rolls, E.T., and Kesner, R.P. (2006). A computational theory of hippocampal function, and empirical tests of the theory. Prog. Neurobiol. *79*, 1–48.

Siapas, A.G., and Wilson, M.A. (1998). Coordinated interactions between hippocampal ripples and cortical spindles during slow-wave sleep. Neuron *21*, 1123–1128.

Skaggs, W.E., and McNaughton, B.L. (1996). Replay of neuronal firing sequences in rat hippocampus during sleep following spatial experience. Science *271*, 1870–1873.

Squire, L.R. (1992). Memory and the hippocampus: a synthesis from findings with rats, monkeys, and humans. Psychol. Rev. *99*, 195–231.

Squire, L.R., and Alvarez, P. (1995). Retrograde amnesia and memory consolidation: a neurobiological perspective. Curr. Opin. Neurobiol. *5*, 169–177.

Teyler, T.J., and Rudy, J.W. (2007). The hippocampal indexing theory and episodic memory: updating the index. Hippocampus *17*, 1158–1169.

Wilson, M.A., and McNaughton, B.L. (1994). Reactivation of hippocampal ensemble memories during sleep. Science *265*, 676–679.

Wouterlood, F.G., Saldana, E., and Witter, M.P. (1990). Projection from the nucleus reuniens thalami to the hippocampal region: light and electron microscopic tracing study in the rat with the anterograde tracer Phaseolus vulgaris-leucoagglutinin. J. Comp. Neurol. *296*, 179–203.

Ylinen, A., Bragin, A., Nadasdy, Z., Jando, G., Szabo, I., Sik, A., and Buzsaki, G. (1995). Sharp wave-associated high-frequency oscillation (200 Hz) in the intact hippocampus: network and intracellular mechanisms. J. Neurosci. *15*, 30–46.